Energetic particle observations from the Ulysses COSPIN instruments obtained during the October–November 2003 events

R. B. McKibben,[1] J. D. Anglin,[2] J. J. Connell,[1] S. Dalla,[3] B. Heber,[4,5] H. Kunow,[6] C. Lopate,[1] R. G. Marsden,[7] T. R. Sanderson,[7] and M. Zhang[8]

Received 6 February 2005; revised 1 June 2005; accepted 15 June 2005; published 27 September 2005.

[1] We report comprehensive observations of solar energetic particle intensities at energies from 0.3 to >100 MeV made by the suite of six Ulysses COSPIN energetic charged particle instruments on the Ulysses spacecraft during the period of intense solar activity in October/November 2003. We also discuss observations of particle anisotropies in selected energy ranges made by these instruments. Located near the orbit of Jupiter and only about 6° north of the heliographic equatorial plane, Ulysses provided important measurements for comparison with 1 AU observations and for assessing the nature of particle propagation in this period of isolated but intense solar activity in the declining phase of the solar activity cycle. The most significant conclusion is that the particle populations in the inner heliosphere were highly nonuniform throughout the events, strongly guided and confined by magnetic structures such as stream interfaces in the solar wind. This provides strong contrast to the nearly uniform intensities that were quickly established after large events near the peak of the solar cycle. Points of particular interest are (1) possible observation at 5.2 AU during onset of differential filling of flux tubes and confinement of high-energy (>∼20 MeV) particles to flux tubes in the course of propagation from the source; (2) apparent exclusion of energetic particles from the interior of a large coronal mass ejection (CME); (3) possible triggered release of electrons from Jupiter by interaction with the same CME, and propagation of the electrons within the closed fields of the CME.

Citation: McKibben, R. B., J. D. Anglin, J. J. Connell, S. Dalla, B. Heber, H. Kunow, C. Lopate, R. G. Marsden, T. R. Sanderson, and M. Zhang (2005), Energetic particle observations from the Ulysses COSPIN instruments obtained during the October–November 2003 events, *J. Geophys. Res.*, *110*, A09S19, doi:10.1029/2005JA011049.

1. Introduction

[2] From the end of October through mid-November 2003, a remarkable series of energetic events occurred on the Sun (see Table 2 of *Lario et al.* [2005] for a comprehensive event list), including the largest X-ray flare ever recorded [*Tsurutani et al.*, 2005]. Most of the activity was centered in a large and complex active region in the southern hemisphere (Region 486) that began producing X class flares almost as soon as it rotated on to the visible face of the Sun on 22 October (see Table 1). Many of these events also produced intense fluxes of solar energetic particles (SEPs), which were observed by spacecraft throughout the heliosphere, including spacecraft near Earth (ACE, IMP-8), in the middle heliosphere (Ulysses, Cassini), and in the outer heliosphere (Voyager 1 and 2). *Lario et al.* [2005] have provided an overall summary of the solar energetic particle observations throughout the heliosphere during this period. In this paper we look in more detail at observations from the Cosmic and Solar Particle Investigations (COSPIN) suite of instruments on the Ulysses spacecraft, which was near 5.2 AU and about 6 degrees north of the heliographic equator during this period. The observations reported here consist of measurements of the intensities and anisotropies of energetic charged particles over the range from 0.3 MeV to greater than 2000 MeV (for protons). In this paper we concentrate on proton observations.

2. Instrumentation

[3] The COSPIN instrumentation has been described in detail by *Simpson et al.* [1992]. Briefly, the COSPIN suite

[1]Department of Physics and Space Science Center, University of New Hampshire, Durham, New Hampshire, USA.
[2]Herzberg Institute of Astrophysics, National Research Council of Canada, Ottawa, Ontario, Canada.
[3]Physics Department, University of Manchester Institute of Science and Technology, Manchester, UK.
[4]Fachbereich Physik, Universitaet Osnabrueck, Osnabrueck, Germany.
[5]Now at Physikalisches Institut, Universitaet Stuttgart, Stuttgart, Germany.
[6]Institut für Experimentelle und Angewandte Physik, Arbeitsgruppe für Extraterrestrische Physik, Christian Albrechts Universität, Kiel, Germany.
[7]Research and Scientific Support Department, European Space Research and Technology Centre, Noordwijk, Netherlands.
[8]Department of Physics and Space Science, Florida Institute of Technology, Melbourne, Florida, USA.

0148-0227/05/2005JA011049

Table 1. Significant Solar Events (M3 or Greater), Days 295–345 (22 October to 11 December), 2003[a]

Day of 2003, Date	X-Ray Max, UT	Class	Location	Region
295 (10/22)	2007	M9.9	S18 E78	486
296 (10/23)	0708	M3.2	N04 E13	484
	0835	**X5.4**	**S21 E88**	**486**
	2004	**X1.1**	**S17 E84**	**486**
297 (10/24)	0254	M7.6	S19 E72	486
	0510	M4.2	S24 E74	485
299 (10/26)	**0654**	**X1.2**	**S14 E44**	**486**
	1819	**X1.2**	**N02 W38**	**484**
	2140	M7.6	N01 W38	484
300 (10/27)	0927	M5.0	S16 E26	486
	1243	M6.7	S17 E25	486
301 (10/28)	**1110**	**X17**	**S16 E08**	**486**
302 (10/29)	0511	M3.5	S17 E06	486
	2049	**X10**	**S15 W02**	**486**
305 (11/01)	2238	M3.2	S12 W60	486
306 (11/02)	**1725**	**X8.3**	**S14 W56**	**486**
307 (11/03)	**0130**	**X2.7**	**N10 W83**	**488**
	0955	**X3.9**	**N08 W77**	**488**
	1532	M3.9	S15 W79	486
308 (11/04)	1022	M3.0		488
	1950	**X28**	**S19 W83**	**486**
309 (11/05)	1052	M5.3	S16 W90	486
310 (11/06)	1730	unknown	backside	
			Fast full halo CME	
311 (11/07)	1554	unknown	backside[b](?)	
			Fast full halo CME	
321 (11/17)	0905	M4.2	S01 E33	501
322 (11/18)	0754	M3.2	N00 E18	501
	0831	M3.9	"	501
	1011	M4.5	"	501
324 (11/20)	0740	M9.6	N01 W08	501
	2354	M5.8	N02 W17	501

[a]Times and locations or solar events obtained from "The Preliminary Report and Forecast of Solar Geophysical Data" published online at http://sec.noaa.gov/weekly/ by the NOAA/SED and the AFWA.

[b]A modest B4.7 X-ray flare, with onset at 1517 and max at 1726 was in progress at CME liftoff, location unknown, but seems unlikely to have generated such a large and fast (>2000 km/s) CME.

consists of six charged particle telescopes, each with a specific measurement focus. Each telescope system was provided by a research group from a different institution within the COSPIN collaboration, and each group has taken primary responsibility for analysis of the data from the telescope it provided. Thus analysis techniques, while similar, are not exactly identical for all telescopes, and differences will be noted when relevant to the discussions in this paper. The charged particle telescopes that comprise COSPIN are as follows:

[4] 1. The High Flux Telescope (HFT) is a very small geometric factor single detector telescope intended to provide measurements of low energy particle intensities (0.3–7 MeV for protons) and anisotropies during periods when the intensities are so high that the larger telescopes in the COSPIN suite approach saturation. The aperture is fan-shaped with the narrow axis in the spin plane to provide 32-sectored measurements of low energy proton intensities. Its threshold of 0.3 MeV is the lowest among the COSPIN instruments.

[5] 2. The Anisotropy Telescope system (ATs) consists of a pair of identical simple 3-detector telescopes inclined at angles of 60° and 145° to the spacecraft spin axis which always points toward Earth. Each AT telescope provides spin-averaged and 8-sectored measurements of the proton intensities at energies from 0.7 to 6.5 MeV.

[6] 3. The Low Energy Telescope (LET) is a multielement dE/dx versus E telescope that provides identification of particle species by pulse-height analysis as well as spin-averaged and 8-sectored counting rates in the energy range 0.9–19 MeV (for protons).

[7] 4. The High Energy Telescope (HET) is a large multielement (13 detectors, six of which are position sensing) telescope aimed at providing extremely high-resolution analysis of the elemental and isotopic composition of galactic cosmic rays. It also provides spin-averaged counting rate measurements of the intensities of energetic charged particles in several energy ranges from ~10 to 92 MeV (for protons) as well as the integral intensity greater than 92 MeV. In addition, 8-sectored counting rates are provided for one energy range each of protons and electrons. The pulse-height analysis capability was designed for studies of galactic cosmic rays, where it provides definitive event-by-event identification of particle species and energy at a low rate, limited by telemetry to one event every 6 s. The counting rates, on the other hand, report numbers of events in broad energy ranges and classes of particle type, counting every event. Thus during high intensity solar particle events the counting rates provide the most useful data from this instrument. While the events under discussion here were large, the intensities were not so high that any major distortion of the logic function from accidental coincidences or saturation effects should have occurred.

[8] 5. The Kiel Electron Telescope (KET) is a sophisticated Cerenkov and solid state detector telescope whose principle aim was to provide measurements of cleanly identified electron intensities and spectra in the energy range ~7–>170 MeV. It also provides measurements of protons in various energy ranges from ~3 MeV to >2 GeV. In addition, 8-sectored counting rates are provided for 5–25 MeV protons and ~3–10 MeV electrons. The Ulysses/COSPIN instrumentation thus provides comprehensive measurements of the energetic particle environment at energies from 0.3 MeV through relativistic energies. As Ulysses provides the only available observations near 5 AU, it is the objective of this paper to present observations of the October–November SEP events over the entire energy range addressed by the COSPIN instruments. The measurements presented are for the most part also available from the Ulysses Data System archive, which can be accessed through the ESA Ulysses Home Page at http://helio.estec.esa.nl/ulysses/.

3. Overview of Observations

[9] Table 1 contains a list of the major events, class M3 or greater, from day 295 through day 345 (22 October to 11 December) 2003, including those responsible for the major SEP events observed throughout the heliosphere. The many X-class events during this period are highlighted using bold-faced type. See *Lario et al.* [2005] for a somewhat more extensive list, which also includes additional details concerning the events.

[10] Figure 1a shows the locations of Ulysses and Earth projected onto the ecliptic at the beginning, middle, and end of the period of major activity, in a frame with the

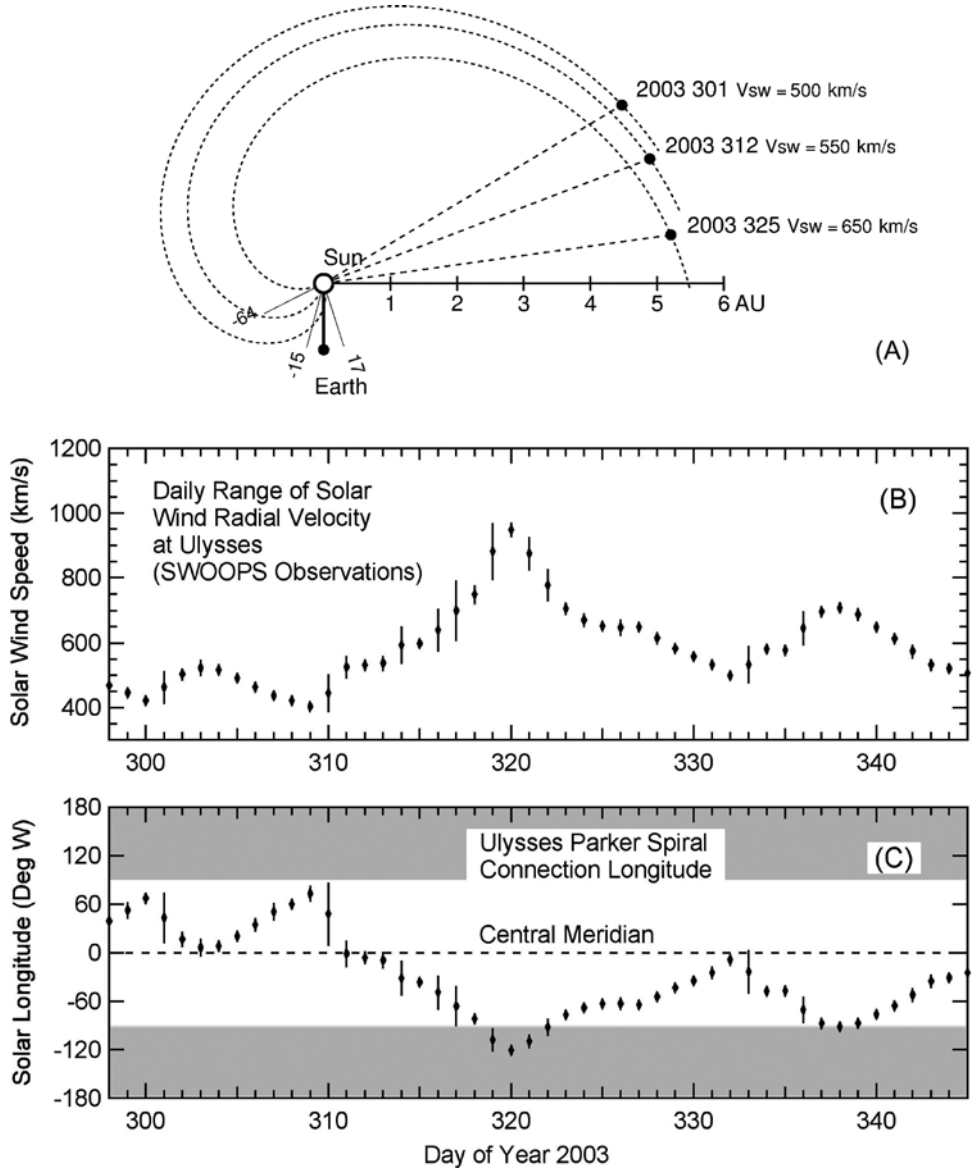

Figure 1. (a) Locations of Ulysses and configurations of the ideal Parker spiral field lines through Ulysses on 3 days during the period of major activity, in a coordinate system with the Earth-Sun line held fixed. (b) Daily range of hourly average solar wind radial speeds at Ulysses measured by the SWOOPS instrument.(c) Ideal Parker spiral connection longitude on the Sun corresponding to solar wind speeds shown in Figure 1b. Longitudes are measured with respect to central meridian as viewed from Earth. Negative values correspond to locations east of central meridian. The invisible hemisphere of the Sun is indicated by shading.

Earth-Sun line held fixed. The ideal Parker spiral magnetic field lines connecting Ulysses to the Sun are also shown, using sample solar wind velocities measured at Ulysses on the three days. Figure 1b shows the daily range of solar wind velocities observed by the SWOOPS experiment on Ulysses, and Figure 1c shows the corresponding longitude range of the foot points on the Sun of the ideal Parker spiral field lines through Ulysses based on the measured solar wind velocities. While in this very disturbed period it is more than likely that the actual field lines are significantly distorted from ideal Parker spirals, the consistency of connection with the visible hemisphere throughout the period even in the face of large variations in solar wind velocity suggests that observations from Earth could be expected to identify the activity that produced any SEPs that arrive promptly by propagation along the interplanetary field. On the other hand, given Ulysses' location somewhat behind the west limb of the Sun, it is quite possible that coronal mass ejections (CMEs) that impact Ulysses might originate on the backside of the Sun and not affect Earth nor be visible from Earth.

[11] The distance along the Parker spiral field lines from the Sun to the Earth was of the order of 10 AU (ranging from ~13 to ~8 AU for solar wind speeds between 500 and 1000 km/s). On day 301, when the major activity began, the solar wind speed was around 500 km/s, implying a field length of 13 AU. Thus onsets should be significantly delayed at Ulysses compared to those observed at 1 AU.

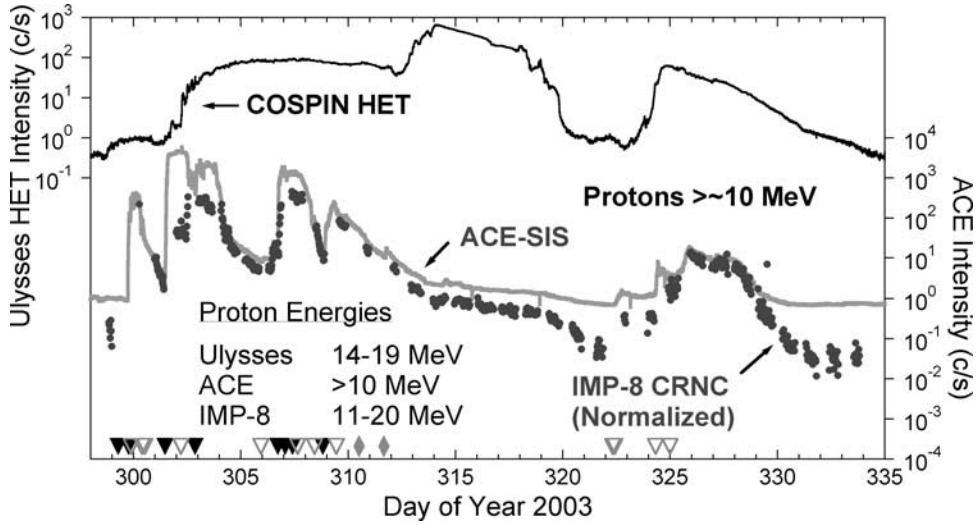

Figure 2. Comparison of intensity profiles of >∼10 MeV protons at Ulysses at 5.2 AU and at ACE and IMP-8 at 1 AU. ACE data are based on counting rates, and the minimum intensity is set by cosmic ray induced background. The IMP profiles are based on identification of particles by PHA. Solid black triangles represent the times of X-Class flares (see Table 1), open gray triangles represent M3 or greater M class flares, and the gray diamonds represent large backside halo CMEs.

Assuming the first arriving particles were accelerated near the Sun, the earliest possible onset time for directly arriving 1, 10, and 100 MeV protons would be ∼39, ∼12, and ∼4 hours after the event, respectively. Fully relativistic particles, such as electrons, could arrive in about 1.8 hours. Thus for particles measured by COSPIN, onset times following a solar event extend over more than a day and a half even for directly arriving particles. As a result, in a period of complex and frequent activity, it might be expected that interpretation of the events will be difficult, an expectation that is amply fulfilled.

[12] Figure 2 shows an overview of observations of >∼10 MeV protons from the Ulysses HET telescope, compared with similar observations from the ACE-SIS and IMP-8 CRNC instruments near Earth. The ACE instrument is described by *Stone et al.* [1998], and the IMP instrument is described briefly by *Garcia-Munoz et al.* [1975]. The Ulysses and ACE observations are based on counting rates, while the IMP-8 observations are based on combined counting rate and PHA information, which is not available from ACE. As a result, the IMP-8 measurements reveal details of the intensity profile at very low levels, when the ACE intensity measurement has already become dominated by cosmic-ray-induced background.

[13] The principle conclusion to be drawn from Figure 2 is that the intensity profiles at 1 and 5 AU were so different as to seem almost unrelated. From day 298 through day 330 there appear to be at least eight significant and distinct particle onsets observed in the ACE data record at 1 AU, compared with four at Ulysses, including the small onset on day 298. In particular, the large event beginning on day 312 at Ulysses, which leads to the highest observed intensity at Ulysses, has no counterpart at Earth. As will be discussed later, it is possible that this event was associated with one of the large backside halo CMEs observed on days 310 and 311 (cf. Table 1). The rise in intensities beginning on day 323 at Ulysses is of uncertain origin. It may be connected to the series of M class events on days 322 and 324 near the center of the visible disk. These events appeared to produce prompt onsets at 1 AU, but, if these same events are the source of the particle intensities at Ulysses, the onset at Ulysses was very gradual and much delayed. This will be discussed further in section 4.4 below.

[14] In all cases, both the rise to maximum and decay of SEP intensities was much more rapid at 1 AU than at 5 AU, and at no point did the intensities at the two locations achieve the near equality and similarity of decay rate characteristic of the so-called "reservoir effect" [*Roelof et al.*, 1992; *McKibben et al.*, 2003] so frequently observed at other times during the Ulysses mission, and particularly when Ulysses was at high latitude near solar maximum. As noted by *Lario et al.* [2005], the period before the October–November events was one of relatively quiet and stable interplanetary structure. The reservoir effects, on the other hand, were generally observed in the very disturbed interplanetary environment characteristic of solar maximum. Further investigation of both current and historical observations is needed to determine whether this is a consistent pattern over many solar cycles.

4. Detailed Observations From Ulysses

4.1. Overview

[15] Figure 3 presents an overview of the proton intensity profiles observed by the COSPIN telescopes in the period 25 October to 11 December (days 298–345), which covers the entire period during which intensities were significantly enhanced following the first large events in late October. As described in more detail by *Simpson et al.* [1992], the view cones of all COSPIN telescopes except for the ATs and HFT are parallel and in the spin plane, normal to the spin axis, which is at all times pointed toward Earth. The AT telescopes are inclined to the spin plane, with Telescope T1 pointing at 60 degrees to the spacecraft spin axis (i.e., in the

earthward looking hemisphere) and telescope T2 pointing at 145 degrees (i.e., in the antiearthward looking hemisphere.) Note that the inclinations of the AT telescopes were inadvertently interchanged by *Simpson et al.* [1992]. The long axis of the fan-shaped HFT viewing aperture is aligned with the spin axis and includes angles between 15° and 75° with respect to the spin axis. The detailed discussions presented in this paper will be limited to days 298–331, slightly before the end of the period of enhanced fluxes from these events. The intensity profiles are based on 10-min averages

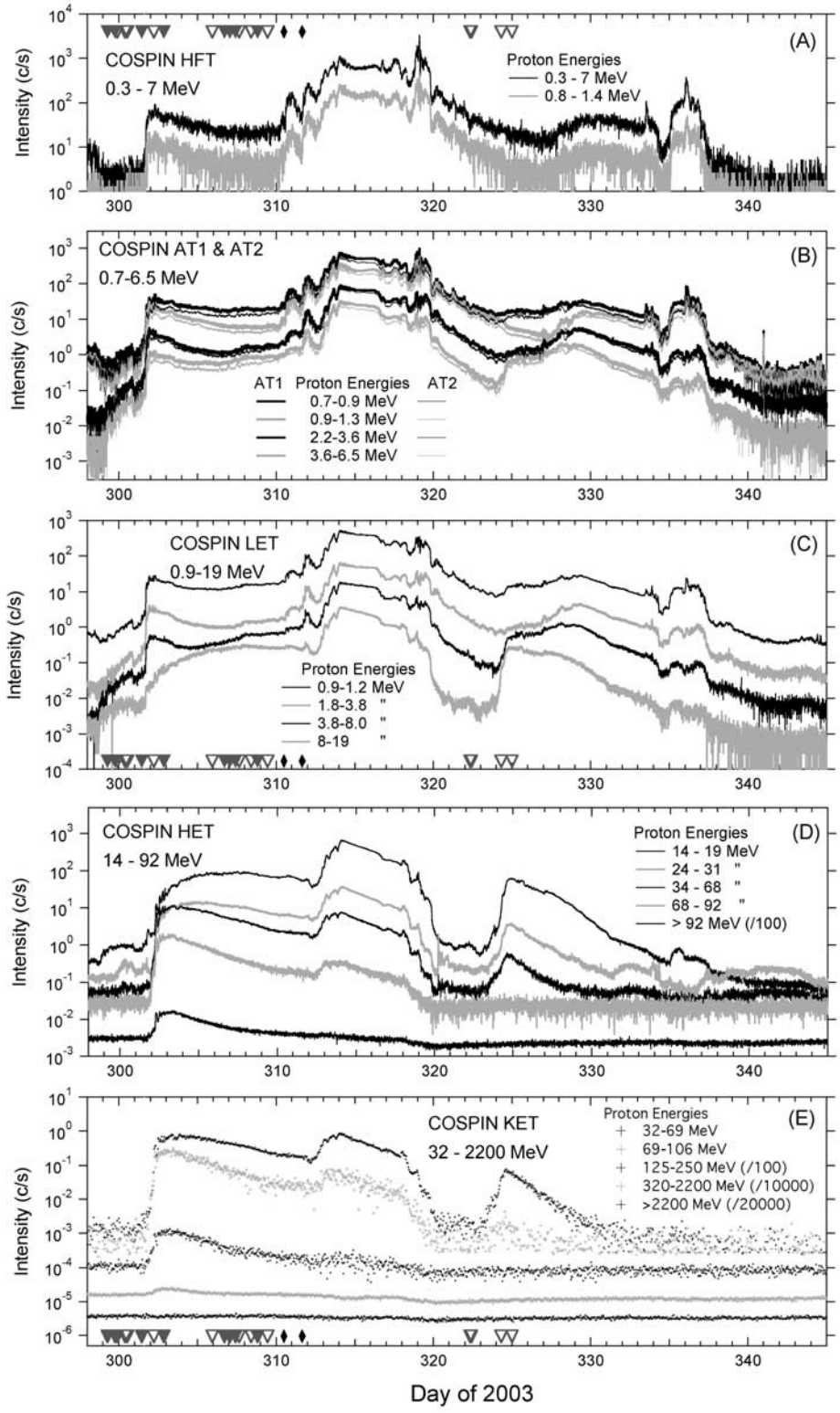

Figure 3

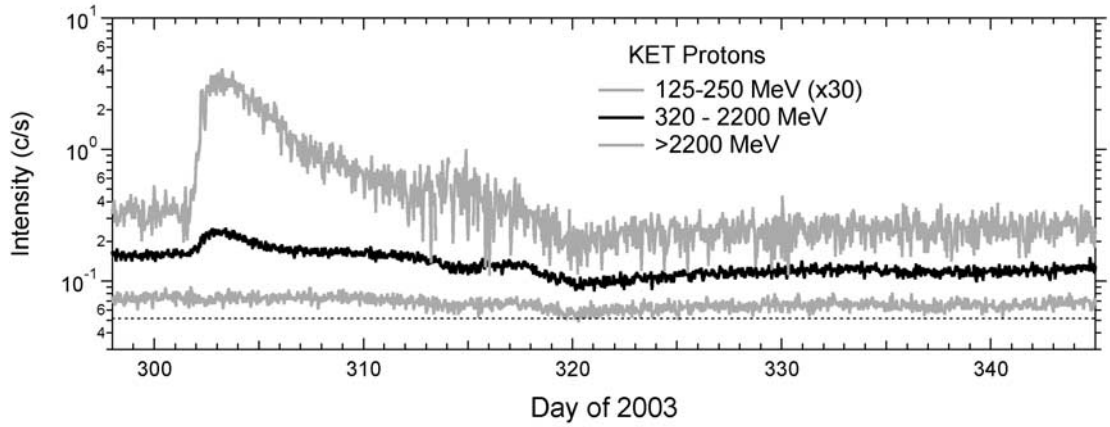

Figure 4. Expanded view of the high-energy proton measurements from the KET.

of the intensities from all sensors except the KET, where hour averages are used, and cover the energy range from 0.3 MeV (from the HFT) through the integral intensity >2200 MeV (from the KET). Solid gray triangles mark the times of X class solar flares, gray outline triangles mark the times of M class flares, and black diamonds mark the times of two large backside full halo CME events (see Table 1). In each panel, the energies measured increase from the top trace to the bottom trace, as indicated by the legends.

[16] Figure 3 confirms the impression, already drawn from Figure 2, that for energies up to about 70 MeV there were basically three large and distinct SEP enhancements at Ulysses during the October–November time period. The first, beginning on day 301–302 in all channels, had the hardest spectrum, with significant enhancements in proton flux extending up to above 250 MeV. The second had a well-defined onset for high-energy particles on day 312 but a much more ragged and complex onset for particles with energies less than about 10 MeV. This second event had a much softer spectrum than the first and, for energies less than about 30 MeV, produced the highest intensities observed during the period shown. However, it did not appear to produce any significant enhancement for protons with energies greater than 125 MeV. The last event, beginning for high energies on day 322, had lower intensity, a very complex behavior as a function of energy, and overall also a soft spectrum, producing no significant increase above about 70 MeV.

[17] To show the highest energy effects more clearly, in Figure 4 we show the KET counting rates corresponding to energies greater than 100 MeV on an expanded scale. While enhanced fluxes of protons were observed above 250 MeV, no enhancement at all is visible above 2200 MeV. A horizontal dashed line at the minimum intensity observed in the period is intended to highlight the existence of a Forbush-like decrease beginning on day 318 and reaching a minimum on about day 320 that can be observed in all of the high energy intensities, corresponding to passage of the shock and CME generated by the flare activity. The effects of the shock and CME are discussed in more detail below.

[18] While the focus of this paper is on proton observations, for completeness we show in Figure 5 electron counting rates from the HET (10-min averages) and from the KET (hour averages) which measure electrons with energies in various energy intervals between ~3 and ~20 MeV. The events were generally not impressive for electrons at these energies. Only the first two events were associated with any significant increase in the electron fluxes, and the fluxes were so low that one must worry about possible contamination of the electron counting rates by misidentified protons. In high rate situations, distortions of the coincidence logic or measured pulse-heights may lead to misidentification of a small percentage of incident protons as electrons, especially in the HET which uses only solid state detectors. Incorporation of Cerenkov detectors in the KET for identification of high velocity particles provides additional protection against contamination, and the agreement in detail between the shapes of the time intensity profiles of the 3–5 MeV electrons measured by the HET with the 3–7 MeV electrons measured by the KET with very different telescope designs [see *Simpson et al.*, 1992] suggests that the identification of these particles as electrons is correct. If this conclusion is valid, perhaps the most remarkable feature of the electron time intensity profiles is their very slow rise to maximum and their close, but not exact similarity to the time-intensity profiles of protons with energies of several 10s of MeV.

Figure 3. Overview of the observations of solar energetic protons from COSPIN instruments during the entire period of significantly enhanced fluxes. This figure is based on 10-min averages of the counting rates prepared for the Ulysses Data System archive, except for the KET, which is represented by hour-average PHA-based fluxes. Within each panel the energies measured increase from the top to the bottom trace, as indicated by the legends. The solid and empty triangles and filled diamonds have the same meaning as in Figure 2. AT1 and AT2 (b) are two identical telescopes inclined with respect to the spin plane, distinguished by solid and dashed (or light) lines. The slight difference between the trace intensities results in part from the Compton-Getting effect in the telescopes inclined radially inward and outwards with respect to the solar wind velocity.

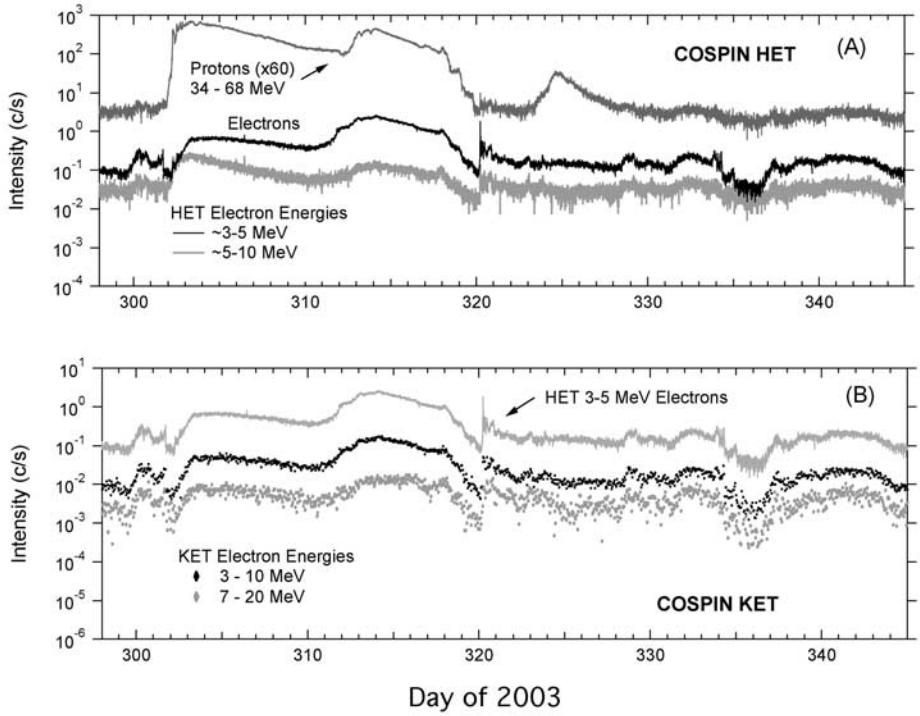

Figure 5. Same as Figure 3, but for counting rates sensitive primarily to electrons.

[19] The sharp electron onset observed on day 320 most likely consists of Jovian electrons. Comparison to proton counting rates allows exclusion of any significant contribution from protons to this increase. In many of the HET proton channels the logic [see *Simpson et al.*, 1992] allows electrons to contribute at levels that are usually negligible but that occasionally, as in SEP onsets or Jovian electron events, become significant. In this case the electrons appear to make a dominant contribution to the normally proton-dominated counting rates, which are at near-background levels. The appearance of the event suggests either a sudden establishment of a good magnetic connection to Jupiter or a burst-like injection from Jupiter along a well-connected field line. If so, it is unusual in that (as will be discussed in section 4.4 below) the onset takes place inside a CME that passed over Ulysses between days 319 and 324. Future papers will present more extensive discussion of Jovian electron observations from COSPIN.

[20] The following more detailed discussion of the observations will focus individually on the most interesting features of each of the three main proton increases observed at Ulysses.

4.2. Onset Phase, Days 300–310

4.2.1. Figure and Format Description

[21] An expanded view of the onset phase of the events is shown in Figure 6. Since this is a complex figure, and since this same figure format will be used to discuss all phases of the event, a brief description of the general format is worthwhile. Specific notations appropriate to the different periods are described in the discussion of that period.

[22] Figure 6a contains counting rate channels from the COSPIN HFT, LET, and HET covering various proton energy ranges between 0.8 MeV and the integral >92 MeV counting rate. Since the emphasis in this panel is on variations of the time intensity profile as a function of energy, the counting rates have been shifted vertically by various arbitrary factors to avoid overlap. Similarly as in Figure 3, the solid triangles (red) mark the times of large X class events. Outlined triangles (blue) and, in later figures, the diamonds (black) also have the same significance as in Figure 3.

[23] Figures 6b, 6c, and 6d present anisotropy information for 1.8–3.8 MeV protons from the LET. Figure 6b contains a color chart representing the ratio of the counting rate in a given sector to the spin-averaged counting rate. Sectors 0 through 7 (on the left axis) each correspond to 45 degree sectors of the spacecraft spin and together span 0–360 degrees in the spin plane, with 0 degrees defined to be the start of sector 0. As shown by the color bar to the right of the panels, the represented sector/spin-averaged range extends from 1.5 (fully saturated red) to 0.5 (fully saturated blue). A ratio of 1.0 is represented by white. Thus a fully isotropic counting rate distribution would plot as white in all sectors with adequate statistics. At low intensity levels statistical fluctuations dominate and the distribution appears as red-white-blue noise. To help assess the alignment of anisotropies with the magnetic field direction, the direction of the measured magnetic field projected onto the spin plane, derived from magnetometer measurements available from the Ulysses Data System (UDS), is plotted using yellow diamonds. At all times during the measurements reported here, the direction of flow outward from the Sun along the nominal Parker spiral lines is near 0 (or 360) degrees. To help associate anisotropy features with features in the time intensity profile, the spin-averaged counting rate for each channel is plotted as the black line, using the right axis for intensity.

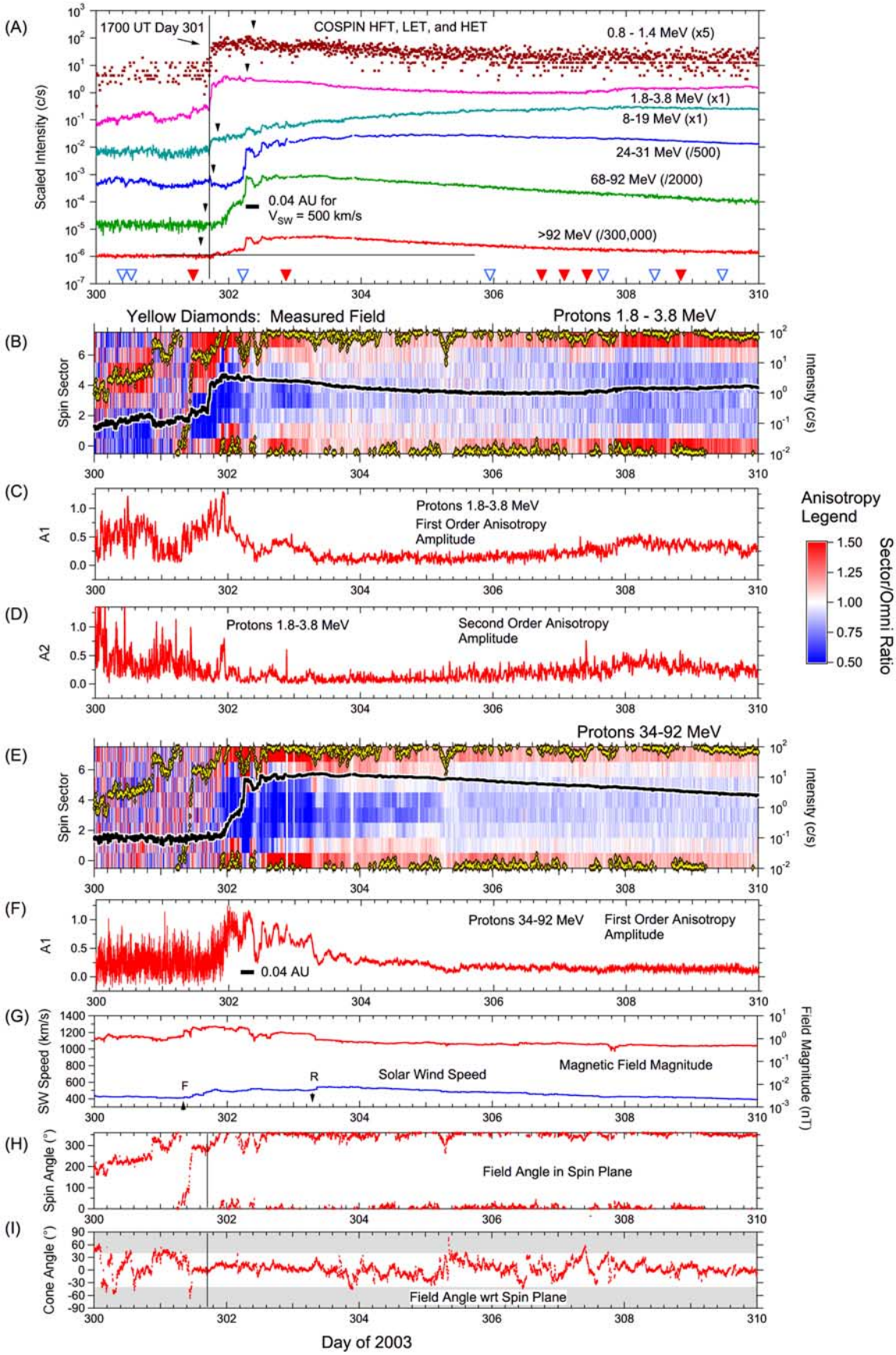
(A)
1700 UT Day 301
COSPIN HFT, LET, and HET
0.8 - 1.4 MeV (x5)
1.8-3.8 MeV (x1)
8-19 MeV (x1)
24-31 MeV (/500)
68-92 MeV (/2000)
>92 MeV (/300,000)
0.04 AU for
V_SW = 500 km/s
Scaled Intensity (c/s)
Yellow Diamonds: Measured Field
Protons 1.8 - 3.8 MeV
(B)
Spin Sector
Intensity (c/s)
(C)
A1
Protons 1.8-3.8 MeV
First Order Anisotropy
Amplitude
Anisotropy
Legend
Sector/Omni Ratio
(D)
A2
Protons 1.8-3.8 MeV
Second Order Anisotropy
Amplitude
Protons 34-92 MeV
(E)
(F)
Protons 34-92 MeV
First Order Anisotropy
Amplitude
0.04 AU
(G)
SW Speed (km/s)
Solar Wind Speed
Magnetic Field Magnitude
Field Magnitude (nT)
F
R
(H)
Spin Angle (°)
Field Angle in Spin Plane
(I)
Cone Angle (°)
Field Angle wrt Spin Plane
Day of 2003

Figure 6

[24] Figures 6c and 6d display the first and second order anisotropy amplitudes in a more quantitative way than is possible with the color chart. These amplitudes, A1 and A2, are the result of a least squares best fit of the angular distribution of counting rates. For the LET, the function used is $F(\theta) = A0(1 + a*\sin(\theta) + b*\cos(\theta) + c*\sin(2\theta) + d*\cos(2\theta))$ where θ is measured with respect to the projection of the magnetic field direction on the spin plane. A1, plotted in Figure 6c, is defined by $A1 = (a^2 + b^2)^{0.5}$, and A2, plotted in Figure 6d, is a similar function of c and d.

[25] Figures 6e and 6f contain the same information as Figures 6b and 6c for the 34–92 MeV protons from the HET, except that here the fit that defines A1 is to the function $F(\theta) = A0(1 + A1\sin(\theta + A3) + A2\sin(2\theta + A4)$, where A1 and A2 are amplitudes and A3 and A4 are phases of the first- and second-order anisotropies, respectively. In this case, $\theta = 0$ corresponds to the start of sector 0. We do not display a panel for the second-order anisotropies since, with few exceptions mentioned briefly in the text below, any significant value of A2 generally shows a close correlation with the value of A1, suggesting that its significance is an artifact of the fit.

[26] Figures 6g, 6h, and 6i, all based on data from the Ulysses Data System, contain the solar wind speed and magnetic field magnitude (G), the angle of the field with respect to the spin plane, referred to as the cone angle (H), and the angle of the field with respect to the sun pulse, projected on the spin plane (I). The shaded regions in Figure 6i indicate the approximate regions where the magnetic field lies outside a 40° acceptance cone normal to the spin axis. This encompasses the view cones of most of the COSPIN telescopes. However, since each telescope has a different acceptance cone, this is meant merely to be a warning rather than a definitive indication that particle flow along the field may not be fully captured by the COSPIN instruments.

4.2.2. Discussion of Onset Observations

4.2.2.1. Onset Times

[27] As shown in Figure 6a, onset of enhanced particle fluxes was observed at all proton energies from 0.8 MeV up through >92 MeV within a few hours of the X17 solar flare observed at 1110 UT on day 301. However, we conclude from the observations that at energies below 20 MeV the particles observed in the early hours following the event were not accelerated in association with this flare. Black triangles mark the earliest expected arrival times for particles propagating from the Sun along the field using the velocity of the highest energy protons contributing to each data channel (the velocity of 300 MeV protons was used for the >92 MeV channel). We have assumed a 13 AU path length along the Parker spiral field, appropriate for the near-500 km/s solar wind speed observed at that time. Comparison of the observed onsets with the expected times shows that the expected velocity dispersion was not observed. Indeed, the onsets for the lowest energy channels were the most abrupt and in some cases occurred well before the onsets of higher energy particles. A line drawn at 1700 UT on day 301 (and extended through other panels of the figure) seems to define a simultaneous onset for the three lowest-energy channels, and perhaps also for the >92 MeV channel (a horizontal line at the background level is drawn to help define the >92 MeV onset). While an onset at 1700 UT is plausible for the >92 MeV particles if they were accelerated in association with the flare, the most likely explanation for the early and simultaneous onset of the low energy particles is that, as a result of corotation, the spacecraft entered a region that was already filled with low energy particles accelerated in a previous event. The solar wind and magnetic field characteristics in Figures 6g, 6h, and 6i show that the onset occurred about 8 hours after a forward shock that initiated a CIR passing over the spacecraft. In fact, *Lario et al.* [2005] have noted that prior to these events a very regular series of CIRs had been observed for at least the previous two solar rotations, and the CIR that enveloped Ulysses during the onset was one that had been observed in the two previous rotations. The leading edge of this CIR occurred in the midst of a rapid 360° rotation of the interplanetary field, but, as discussed below, we do not believe that this rotation is significant for the timing of the onset.

[28] In Figure 7, we show the solar wind Vr, Vt, and Vn components, along with the proton density and temperature, derived from high resolution SWOOPS data available from the Ulysses Data System. The high-resolution data during this period provides 8-min averages of the solar wind properties. For comparison, 10-min averages of the 1.8–3.8 MeV proton intensity are also shown. The proton onset at 1700 UT is marked by vertical lines in all panels. Even though, as shown in Figure 6g, there was no strong signature in the solar wind radial velocity or magnetic field to mark the onset, it appears to be closely associated with a deflection in the solar wind speed indicated by increases in the Vt and Vn components, and with a spike in the temperature. The maximum deflection was approximately 16 degrees from the radial direction. These observations suggest that the onset may be coincident with an interface in the CIR between plasmas with different origins, possibly the

Figure 6. Observations during days 300–310. See section 4.2.1 for a more detailed description of the format. The solid vertical lines indicate the onset time of ~1 MeV protons. (a) overview for several energy channels from 0.8–>92 MeV protons. Black inverted triangles represent the earliest possible arrival of particles in the respective energy channels propagating along interplanetary field lines. Solar events are represented as in Figure 3; (b) Omidirectional intensity (black line, right axis) and ratio of intensity in spin sector (left axis) to the spin-averaged intensity (color legend to right) for 1.8–3.8 MeV protons. The start of sector 0 defines 0° in these spin plane coordinates. Yellow diamonds indicate the measured field direction projected on the spin plane. The nominal Parker spiral lies near 0° during this period; (c) and (d) Amplitudes of the first and second order anisotropies corresponding to the observations in panel B; (e) and (f) Same as B and C for 34–92 MeV protons; (g) Solar wind radial velocity (left axis) and magnetic field magnitude (right axis) from the Ulysses Data System Archive. In this and all figures Forward (F) and Reverse (R) shocks are indicated by black triangles; (h) Cone angle of magnetic field (angle with respect to the spin plane). Grey bars indicate regions that lie outside a 40° view cone oriented normal to the spin axis. (i) Magnetic field direction projected on the spin plane (same as yellow diamonds in B and E).

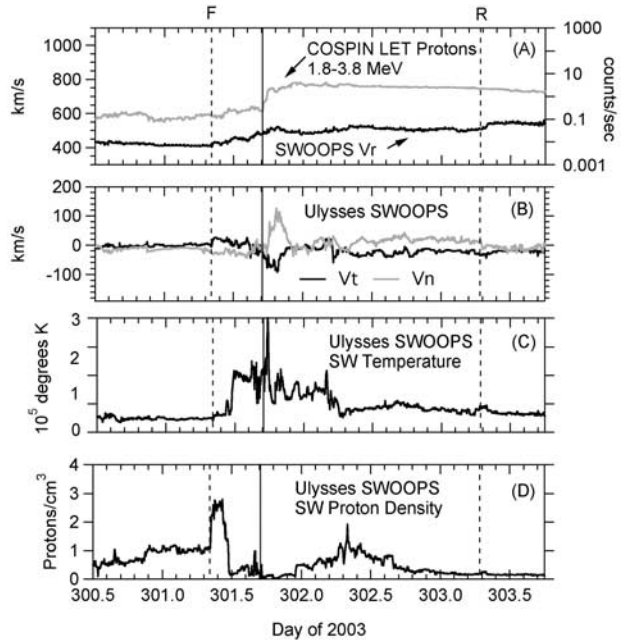

Figure 7. Eight minute average observations of solar wind V_r (A), V_t and V_n (B), temperature (C), and density (D) from the Ulysses SWOOPS instrument. The velocities are measured in the RTN system where r points radially outward from the Sun, t points in the azimuthal direction in the sense of the solar rotation, and n completes a right-handed system. The vertical line indicates the onset time for low energy protons (gray curve in panel A, consisting of 10-min averages) and shows correlation with a feature that may represent the stream interface in a CIR passing the spacecraft during this period. Data are from the Ulysses Data System archive. The dashed lines represent the forward and reverse shocks that bound the CIR (J. T. Gosling, private communication, 2004).

interface between the solar wind flows that gave rise to the CIR. As summarized by *Crooker et al.* [1999], the classic CIR stream interface is defined by a number of characteristics. It is not the purpose of this paper to give a detailed diagnostic of the solar wind structures in this event, which would constitute an interesting research topic in itself. However the observations in Figure 7 strongly suggest an interface between two dynamically interacting plasma streams. If so, it is plausible that the streams have significantly different origins on the Sun so that field lines on one side might be filled with low-energy SEPs while field lines on the other side of the interface might be relatively empty of SEPs.

[29] Determination of the source of the particles confined behind the interface is not straightforward. Prior to the day 301 event the largest events were two X1.2 events recorded on day 299, one at S14 E44 at 0654 UT from region 486, and one at N02 W38 at 1819 UT from region 484. Both were accompanied by large and fast partial halo CMEs (http://cdaw.gsfc.nasa.gov/CME_list/UNIVERSAL/2003_10/univ2003_10.html). As shown in Figure 2, ACE recorded a clear and abrupt onset associated with the second event, and no increase associated with the first, not surprising considering their positions relative to Earth. Ulysses saw no prompt increase from either event, despite the fact that on day 299 its connection longitude was in the range ~40–60° W (cf. Figure 1), which would normally be well positioned to see particles from the event. There is no obvious reason why Ulysses should not have seen particles from this event, but it did not.

[30] As shown in Figure 7, on day 301 the solar wind speed increased from ~410 km/s to ~520 km/s during the day, which corresponds to a range of connection longitudes, shown in Figure 1, decreasing from about 75°W on the Sun in the slow wind at the start of the day to 10°W at the end of the day. The wind speed at the interface, about 480 km/s, corresponds to a connection longitude of about 25°W. Two days earlier on day 299 therefore the longitude range of the same sources of wind on the Sun would have been between ~45°W and ~20°E, with the connection longitude of the interface just east of Central Meridian. Thus at the time of the W38 event, the connection longitude corresponding to the interface would have been east of the event at W38 and well east of the ACE connection longitude but west of the event at E44. If the event at E44 produced large numbers of energetic particles, and if the stream interface acted as a strong boundary, neither ACE nor Ulysses was in position to observe them. The stream interface rotated past Ulysses on Day 301, producing the particle onset, when ACE was still on the other side of the stream interface. When about 2 days later the interface rotated past Earth, fluxes from the day 301 event and another event late on day 302 may have covered any increase in flux from particles left over from the day 299 event. Thus even though the picture is not fully consistent and coherent (there is still no clear explanation of why Ulysses did not see particles from the W38 event on day 299) we tentatively suggest that the onset observed at ~1700 UT on day 301 consisted of particles accelerated in the event from region 486 recorded on day 299. The generally rising intensity and outward particle flow along the field observed at low energies prior to the day 301 onset (Figure 6b) may then be understood as a result of particles that have leaked through the barrier onto field lines that intersect Ulysses.

[31] If this suggestion is correct, then no definitive onset of particles from the day 301 event was observed at Ulysses at any proton energy less than about 10 MeV. As shown in Figure 6a, at energies above about 20 MeV, plausible if slightly delayed onsets were observed, accompanied by strong outward flow (Figures 6e and 6f), which can probably be attributed to the day 301 event.

4.2.2.2. Unusual Intensity Variations During Onset

[32] A particularly interesting feature of the onsets at high energies is the oscillatory nature of the rising intensities on day 302, clearly apparent in the intensity profiles of counting rates covering energy ranges from 8 to >92 MeV in Figure 6a. The variations were simultaneous in all channels. Since particle velocity increases by a factor of more than three from 8 MeV to 92 MeV, the simultaneity excludes time dependent injection and/or propagation effects as the cause for the variations. As shown in Figures 6e and 6f, which display anisotropy information for 34–92 MeV protons, the intensity oscillations were also accompanied by changes in the first order anisotropy amplitude. Figures 6h and 6i show that similar variations were also

visible in the field direction. The change in field direction was about 135° in the first and largest of the oscillations. As shown by the black horizontal bars in Figures 6a and 6f, the spatial scale of the oscillations was about 0.04 AU, assuming they represent convected intensity structures and using the roughly 500 km/s solar wind velocity observed at the time. In the magnetic field observed at the time ($\sim 2 \times 10^{-5}$ gauss), this corresponds to about 10 gyroradii for a 70 MeV proton.

[33] In both appearance and spatial scale, these observations are very reminiscent of those reported by *Mazur et al.* [2000] concerning intensity ''dropouts'' of low-energy particle fluxes during impulsive particle events observed at 1 AU. The suggested interpretation by Mazur et al. was that this represented differential filling of flux tubes which, while adjacent at the point of observation, had significantly different connections to the point of acceleration as a result of random walk of fields in the course of the time required for the solar wind to propagate from the Sun to 1 AU. The same interpretation is difficult to sustain for these observations.

[34] First, the scale over which the effect is observed is much larger. Ulysses was at 5.2 AU from the Sun, and the path length along the average Parker spiral field from the Sun to Ulysses was about 13 AU. This requires extremely good confinement of particles to individual flux tubes for more than 20 hours as they propagate from the point of acceleration. Since the scale of the fluctuations is only about a factor 10 greater than the gyroradius of the 70 MeV protons, almost unreasonably tight confinement of the particles by the field would be required.

[35] Second, Mazur's observations were of low-energy particles from an impulsive event. Such events are usually thought to result from highly localized acceleration and injection at the Sun, producing large intensity gradients across the injection region. The observations reported here refer to a gradual event, where according to current models acceleration occur at a shock driven by a rapidly expanding CME, with only relatively small gradients in intensity or effectiveness of acceleration along the shock front. The CME produced by this event was extraordinarily fast and strong, described colloquially as ''the mother of all halos'' in the LASCO CME list (ftp://lasco6.nascom.nasa.gov/pub/lasco/status/LASCO_CME_List_2003). It was launched at 1054 UT on day 301, and in only a little more than half an hour it had expanded to a full halo. It still had a speed of more than 1850 km/s when it passed Earth on day 302 [*Skoug et al.*, 2004]. The particles observed during the onset were most probably accelerated during the early phases of the event, when it was still near the Sun. It is thus possible that the spatial gradients in the intensity of accelerated particles were sufficiently large that differential connection of flux tubes to the acceleration region as a result of random walk of fields (scale of a few degrees) could explain the observations. However, the rapidity with which the CME developed and expanded makes this interpretation difficult to accept.

[36] An alternative interpretation might be that the propagation characteristics in adjacent flux tubes were sufficiently different that particles arrived more quickly in some than in others. Such propagation discrepancies have been suggested by *Zimbardo et al.* [2004] and *Ruffolo et al.* [2003] as possible alternative explanations for Mazur's observations. In fact similar observations of intensity fluctuations during onsets of SEP events, primarily at lower energies, have been reported by *Sanderson et al.* [2000], where the intensity changes were found to be associated with passage of magnetic discontinuities, which might be interpreted as boundaries of flux tubes. *Sanderson et al.* [2003], examining a similar case of a low-latitude onset at low-latitudes during passage of a CIR, also conclude that there were channels within the structure through which particles propagate more rapidly than in others.

[37] As a final alternative, the quasi-periodic nature of the intensity variations and of the magnetic field deflections, both with a period of about 5 hours, suggests that large-scale waves in the interplanetary field may also play a role. The variations are roughly in phase with maximum anisotropy amplitude correlated with the dips in the magnetic field spin angle toward 300° shown Figure 6h. However, analysis of the magnetic field data for the presence of waves is beyond the scope of this paper. Even if the field observations are consistent with waves, it is not clear how they might lead to the intensity variations.

4.2.3. Observations at Late Times After Injection (Days 305–310)

[38] For the remainder of the first phase of the event up through day 310, little further development is obvious. The intensities with threshold energies above about 10 MeV exhibited smooth decay, with, as shown for the 34–92 MeV protons in Figure 6, modest outwardly directed anisotropies along the relatively quiescent interplanetary magnetic field. At lower energies, following an initial period of intensity decay to a broad minimum centered approximately on days 305–306, intensities began to increase gradually (see Figure 3 as well) as did the anisotropy amplitude. On day 307 a small but noticeable increase in intensity and anisotropy amplitude occurred, perhaps as a result of a fresh injection of particles from a series of X class events beginning on day 306, or, as pointed out by a referee, possibly from particles streaming outward from the forward shock that arrived on day 310. However, as shown in Figure 8, only a modest intensity increase was directly associated with passage of the shock. No similar signatures were observed at energies >20 MeV.

4.3. Midphase Observations: Days 310–322

[39] Observations during the mid-phase of the events, including the second of the three major SEP events observed at Ulysses, are presented in Figure 8, which is in the same format as Figure 6, described above.

[40] At the start of day 310, the intensities at low energies were rising or steady, while intensities at energies greater than 20 MeV were declining. Anisotropies were moderate (1.8–3.8 MeV protons) or small (34–92 MeV protons) and outwardly directed along the field, which had been relatively quiet and stable for many days. This pattern was disrupted at 1648 UT by a forward shock which initiated a period of intense interplanetary disturbance, leading up to passage of a CME starting late on day 319, as indicated by the blue bar in Figure 6g. (Times of all shocks and other disturbances during the period are taken from *de Koning et al.* [2005]). While the higher energies were little affected by this shock, at about

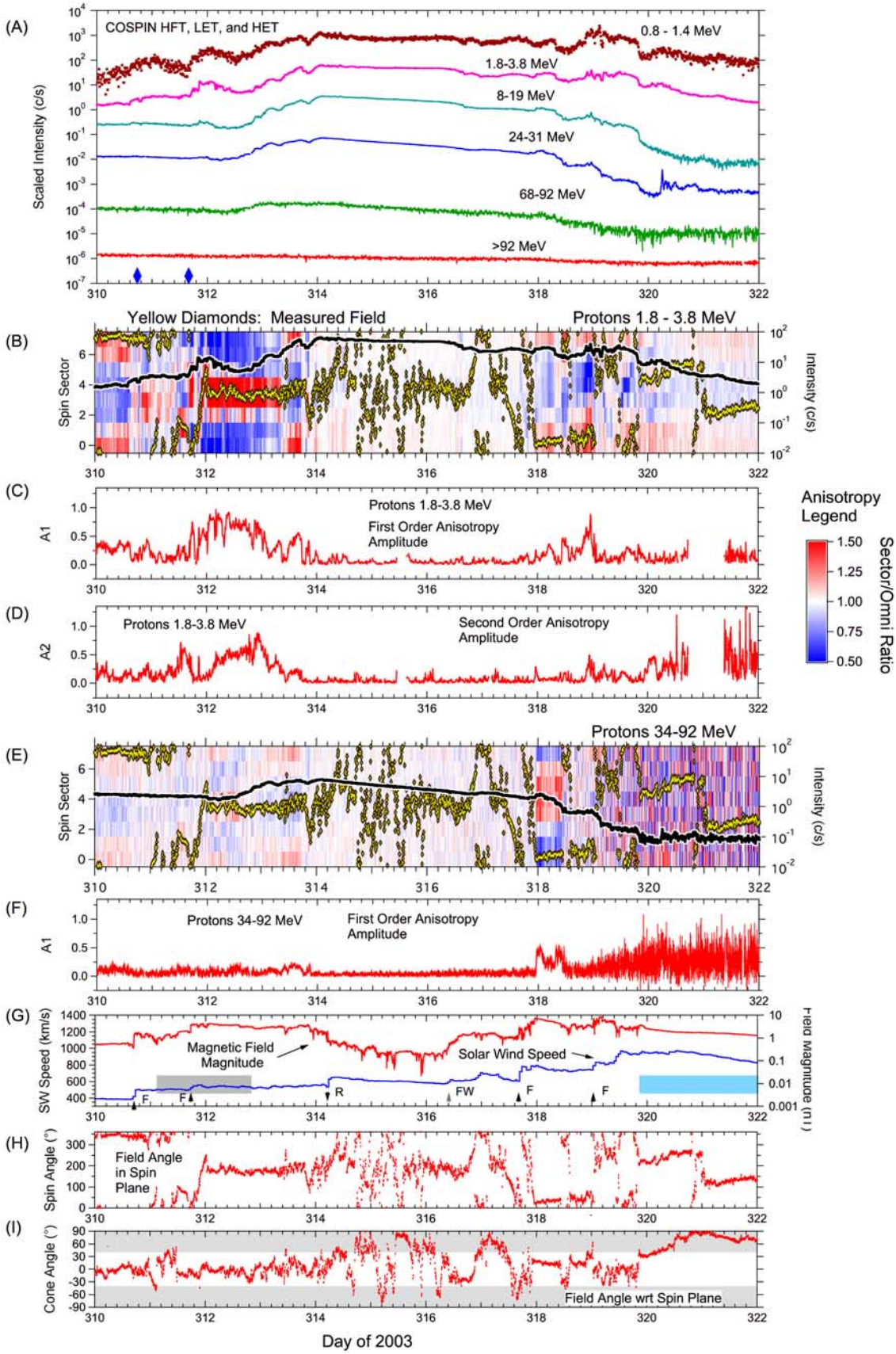

Figure 8. Same as Figure 6 for days 310–322. Gray and blue bars in the solar wind-magnetic field panel represent possible and definite CME periods [*de Koning et al.*, 2005]. FW in panel G identifies a Forward Wave.

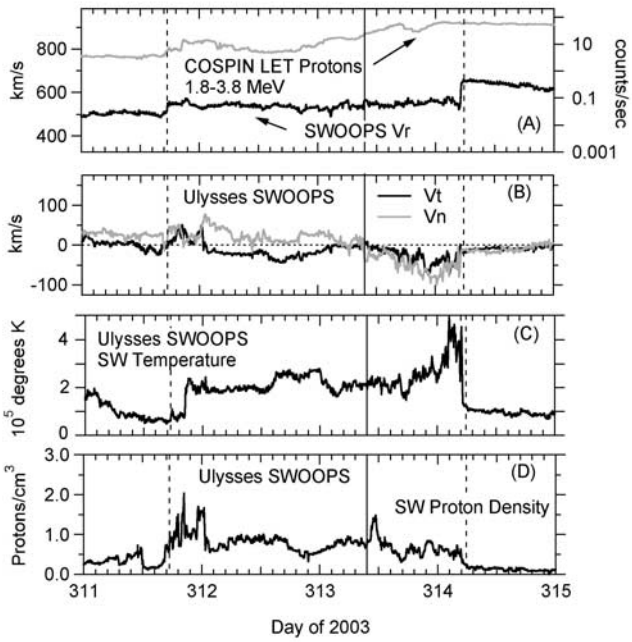

Figure 9. Same as Figure 7 for the period days 311–315. Vertical dashed lines represent the bounding shocks of a CIR, and the solid vertical line represents a possible stream interface.

1600 UT on day 310 the low-energy anisotropy reversed, apparently slightly before the passage of the shock, so that particles flowed inward toward the Sun along the field. With brief interruptions for about an hour near ~1900 UT day 310 and for several hours beginning near noon on day 311, this flow was maintained until about 0900 on day 313. The natural explanation, as suggested by *Lario et al.* [2005] for comparable energy observations from the HI-SCALE instrument on Ulysses, is that the particles were accelerated at the shock and flowing away from the shock both upstream and downstream. Although *Lario et al.* [2005] observed significant intensity increases at lower energies associated with the shock, there was little intensity change at COSPIN energies associated with passage of the shock. A complicating factor is the passage of a possible CME between 0245 UT on day 311 and ~2000 UT on day 312 [*de Koning et al.*, 2005], as indicated by the grey bar in Figure 6g. There are, however, no significant features in the particle intensity or anisotropy that correlate with the suggested boundaries of this CME. More effective was a second forward shock at 1731 UT on day 311, after which the field regained a stable orientation, and the inward flowing anisotropy strengthened markedly for the low-energy protons. *de Koning et al.* [2005] suggest that this shock and the reverse shock that followed at 0508 UT on day 314 form the boundaries of a CIR apparently partially overtaken by the proposed CME.

[41] For almost the entire time that the spacecraft was in the CIR, the first-order anisotropy for the low-energy protons was inwardly directed along the field, consistent with flow away from the forward shock that passed the spacecraft on day 311. At the same time, the second-order anisotropy was enhanced throughout most of the CME passage, and even persisted after the end time for the CME suggested by *de Koning et al.* [2005]. However, close examination of the sector plot (Figure 6b) shows only two brief periods of bidirectional flow during this period, namely from approximately day 311.5–311.7 and from day 312.9–313.4, when two minima and a primary and secondary maximum are observed in each in the 8 sectors. For most of this period therefore we consider the enhanced second-order amplitude as most likely an artifact of the fitting procedure rather than a true indication of bidirectional flow. At about 1000 UT on day 313 the net flow switched direction for about 6 hours and became again directed outward from the Sun. As shown in Figure 8, this change in flow occurred about an hour before a brief deflection of the magnetic field direction. Figure 9 shows that at the same time as the field deflection there was a local maximum in the solar wind density and a significant change in solar wind flow direction, suggesting again the possible passage of an interface between plasmas of different origin inside the CIR. While this transition does not show many of the characteristics of a principal CIR stream interface as described by *Crooker et al.* [1999], the behavior of the Vt and Vn components appears almost identical to that shown in their Figure 2 as a typical stream interface crossing. After crossing the possible interface, the new flow direction of the energetic particles became consistent with flow from the approaching reverse shock. However, shortly before the end of day 313, a few hours before the passage of the reverse shock and approximately coincident with a major deflection of the magnetic field direction, the anisotropy abruptly disappeared. After this change, the magnetic field changed character, weakening toward the reverse shock and becoming highly variable.

[42] Throughout this time, the high-energy proton anisotropy shown in Figure 8 was very weak, but also complex. At times it was bidirectional (e.g., from about day 312.1 –312.6 as shown in the 34–92 MeV proton sector plot in Figure 8), but in general it was consistent with the picture derived from the lower-energy anisotropies, demonstrating flow away from the shocks within the CIR, a change from inward to outward flow at the suggested stream interface, and an abrupt disappearance at the end of day 314.

[43] Following passage of the CIR, the proton fluxes at low- and high-energy became nearly isotropic. At energies below about 30 MeV the intensities immediately after passage of the reverse shock were the highest observed during the October/November series of events. As shown in Figure 3 (bottom panel) and Figure 4 a small intensity increase was observed even in the KET 125–250 MeV proton channel. Such high energies make it very unlikely that the CIR shocks were the source of the particles observed. A more likely source for the particles is one of the large backside halo CMEs observed on days 310 and 311, which are marked by the diamonds in the top panel of Figure 8. Whichever CME might be the source, a significant delay is required for arrival the high energy protons at Ulysses. For example, with the CME liftoff at about 1554 UT on day 311 (311.663) 92 MeV protons propagating along the roughly 12.3 AU Parker

spiral field line implied by the ~530 km/s solar wind speed at the time could have reached Ulysses by day 311.9. However, the flux increase did not begin until approximately day 312.4, half a day later. Also puzzling is the fact that the anisotropies continued inwardly directed during the apparent onset. It is likely that the CME enveloping the spacecraft at the time may have had a controlling influence on both the apparent onset time and the anisotropy direction, but a fully consistent picture has yet to be developed.

[44] Following passage of the CME/CIR combination, the intensities at all energies decayed slowly and smoothly until arrival of a forward shock on day 317. During this whole period, the magnetic field was weak and highly variable in direction. The extreme isotropy and smoothness of the time intensity profiles may be the result of increased diffusion acting to smooth out particle gradients in this region of very irregular magnetic fields. Alternatively, it may be the result of confinement of the particles in a bottle-like configuration of weak fields sandwiched between the strong fields of the CME that had just passed and the strong fields associated with, first, the forward wave [*de Koning et al.*, 2005] observed on day 316, and the even stronger fields observed following the forward shock at about 1600 on day 317.

[45] Beginning shortly after the forward wave at about day 316.4, the magnetic field direction began a remarkable series of gyrations, including more than two complete rotations in the spin plane. Starting at ~316.5, the field first rotated ~180° in the direction of the spacecraft spin, moving from sector 3, through sector 7 to sector 0, then reversed its rotation and, between 317.0 and 317.6, rotated through 360° in the opposite sense. Immediately before arrival of the forward shock at 317.67, the field reversed rotation again, rotating more than 90° in the direction of the spacecraft spin. Immediately after passage of the shock it reversed yet again and rotated rapidly through almost 500° before adopting a stable orientation at about 317.95. During the last rotation, except for a brief period of chaotic field orientation centered at 317.88, weak anisotropies aligned with the field were observed for both low and high-energy protons. At the end of the rotation, the magnetic field magnitude was a near its maximum value during the entire sequence of events. The time of maximum field magnitude marked the return of significant anisotropies in the particle flow and the beginning of a steep decline in the intensities at all energies above ~10 MeV. Remarkably, the anisotropies for 1.8–3.8 MeV protons and 34–92 MeV protons were oppositely directed, outward along the field at low energies, and inward for the higher energies. No interpretation is immediately apparent. For 34–92 MeV protons, the anisotropies were terminated by a rapid change in direction of the magnetic field at about noon on day 318. At lower energies, the 1.8–3.8 MeV proton anisotropies continued until arrival of a strong forward shock at 0033 UT on day 319. The anisotropy amplitude increased dramatically in the hours before the shock arrived, suggesting continuing acceleration at the propagating shock front.

[46] The shock on day 319 presaged the arrival of a very large and fast CME which *de Koning et al.* [2005] conclude corresponds to a large and very fast halo CME launched from just behind the west limb of the sun at 1554 UT on day 311. This CME dominated the last phase of the October/November SEP events as observed at Ulysses, discussed in the following section.

4.4. Late Phase Observations, Days 319–331

4.4.1. CME Passage and Its Effects on SEP Intensities

[47] Figure 10 presents observations for the period from day 319–331, slightly overlapping with the period shown in Figure 8, and continuing through passage of the CME and for several days beyond. Observations related to passage of the CME were by far the most significant aspect of this period.

[48] On the basis of a variety of plasma and magnetic field characteristics, *de Koning et al.* [2005] have placed the onset of the CME at about 2030 UT on day 319. They find, however, that time of termination was ambiguous. Some signs, in particular a sudden change in the magnetic direction and the cessation of bidirectional streaming of suprathermal electrons, indicate that the CME terminated at about 0400 on day 324, while others suggest that the spacecraft was still inside the CME until about 1200 on day 325. The blue bar and the narrower gray bar in the solar wind speed/magnetic field magnitude panel (G) of Figure 10 indicate certain duration of the CME and the period of ambiguity, respectively.

[49] In the energetic proton intensity profiles shown in Figure 10, the onset of the CME coincided with a sharp decrease in intensity at all energies from 0.8 MeV up through 68–92 MeV, where a small but still discernable decrease was observed. At the highest energies (e.g., >92 MeV protons in Figure 3d), the intensities began to increase again after the initial decrease, but for the particles below about 10 MeV the intensity decline continued throughout passage of the CME. For protons above ~10 MeV the intensities declined nearly to background levels. At lower energies intensities reached a local minimum near the end of the CME.

[50] As shown in Figures 10b, 10c, and 10d little effect on first-order anisotropies was observed for the low-energy (1.8–3.8 MeV) protons, but the second-order anisotropies were enhanced through most of the CME passage. For the most part the particle flow remained essentially unidirectional. However, closer examination of the observations presented in Figure 10b shows evidence for sporadic but generally weak bidirectional flow during the CME period. Even on the compressed scale of Figure 10, bidirectional flow is clearly visible in the periods day 320.0–320.15 and day 322.15–322.4.

[51] During the ambiguous termination of the CME, the energetic particle data, not considered by *de Koning et al.* [2005] in their description of this period, provide some additional information.

[52] At the first suggested time for termination of the CME, 0400 UT on day 324, the intensity of 1.8–3.8 MeV protons was near its minimum value during the period shown in Figure 10. For proton energy channels above about 10 MeV, where significantly enhanced fluxes were observed the intensities were rising toward a broad local maximum observed near 1800 UT on day 324. For 8–19 MeV and 24–32 MeV protons, the slope of the intensity rise increased significantly for several hours after passage of the possible boundary of the CME at 0400 UT, leading to a shoulder on the ongoing rise toward the local

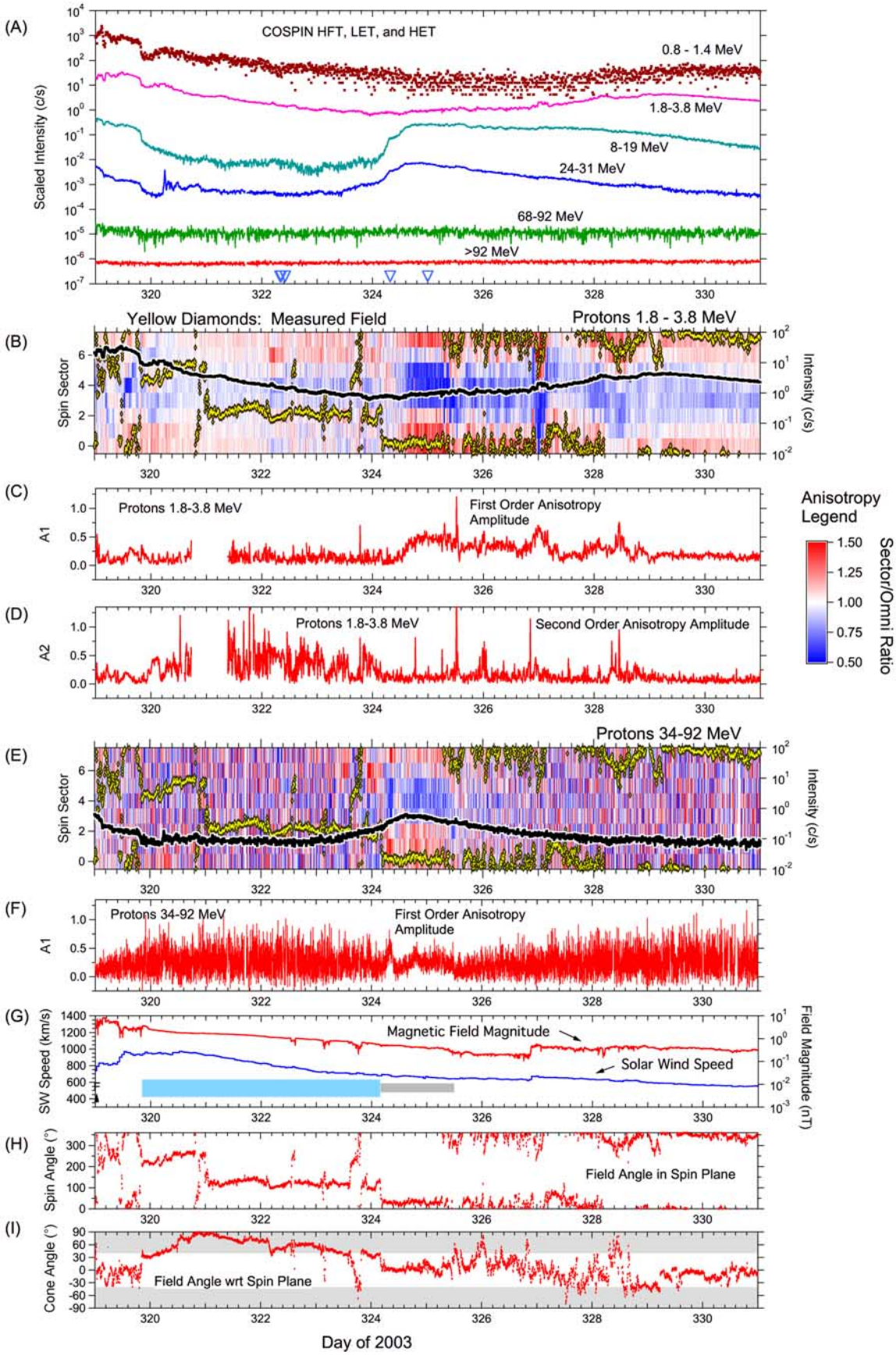

Figure 10. Same as Figure 6 for the period days 319–331. The gray and blue bars have the same meaning as in Figure 8.

maximum. For the 34–92 MeV protons, a very gradual increase in intensity began around midday on day 323, accompanied by a generally outward flow of particles along the field. Late on day 323 the field direction changed dramatically for a period of about 5 hours, after which the preexisting flow was reestablished. After a brief period of bidirectional flow from ~0000 to ~0400 UT on day 324, outward flow along the field was again observed and the increase in intensity became more rapid. The outward flow persisted through the maximum intensity observed during this period and on to the end of the period of ambiguity at about midday on day 325. For the lower energy, 1.8–3.8 MeV protons, no immediate effect on the anisotropies was observed at the time of the suggested boundary at 0400 UT, but a significant outward flow began about 8 hours later, roughly coincident with the very poorly defined start of a gradual increase in intensity from the local minimum level observed earlier on day 324.

[53] At the second suggested time for termination of the CME, 1200 UT on day 325, little effect was noted on the intensities of protons of any energy, but the outward flow ceased for the 34–92 MeV protons and diminished significantly for 1.8–3.8 MeV protons.

[54] While there is much detail that is difficult to understand, especially in the particle flows, a principal conclusion suggested by the observations shown in Figures 3 and 10 is that surrounding particle populations are excluded from the interior of the CME, as indicated by (1) the abrupt decrease in particle intensity observed on entry into the CME, with continuing decline toward the interior, clearly suggesting that the leading edge of the CME constituted a leaky barrier to particle propagation; (2) the gradual increase in intensity toward the end of the CME, coupled with the rapid intensity increase observed when the spacecraft left the closed-field-line structure of the CME, is again consistent with the trailing edge of the CME acting as a leaky barrier; (3) the less than ~6 hours difference between the times of maximum (at high energies) or the ledge at the end of the rapid particle increase (at low energies), over the range of energies measured, from ~ 1 MeV through >34 MeV suggests that the initial intensity increase was the result of entering a region already filled with energetic particles rather than the simple arrival of a newly accelerated population.

[55] The next question is whether the particle intensities observed after the passage of the closed-field-line region of the CME should be attributed to a fresh injection of particles from the Sun, or whether they might be part of a single enveloping population of solar energetic particles observed both before and after but excluded from the interior of the CME. On the basis primarily of the reestablishment of outward flow after passage of the CME, *Lario et al.* [2005] suggest that the increase represents a fresh injection from the Sun, with the onset possibly obscured by suppression of intensities inside the CME.

[56] Suggestive of a common source for protons before and after the CME is that for all proton energies the maximum intensity reached after passage of the CME was within about a factor 3 of the intensity predicted by extension of the trend line established during the decay from day 314 through day 317 prior to passage of the CME. This is best seen by reference to Figure 3. However, the same observations also provide perhaps the strongest observational argument against this hypothesis since, especially at high energies, the maximum intensities observed after the CME were up to a factor 3 higher than the trend line.

[57] Whatever the source of the particles observed after passage of the CME, both interpretations suggest effective exclusion of the surrounding particle populations from the interior of the CME, which is our principal conclusion from these observations.

[58] As noted above, beyond about day 325 the situation remains confused. As shown in Figure 10, just before the end of day 326 a possible shock passed the spacecraft, and at all energies below about 10 MeV the particle intensities began to increase toward broad maxima which showed a clear energy (or velocity) dispersion. Times of maxima extended from about day 328 for 8–19 MeV protons to sometime on day 330 for ~1 MeV protons. Two possible interpretations can be suggested. One is that the rise to maximum intensity represents a continuing recovery from the depletion of particles by the CME. The successively later maxima toward lower energy then imply either an energy dependent zone of exclusion behind the CME or an energy dependence in the time required for the particles from the enveloping population of SEPs to diffuse into and replenish the region swept of particles by the CME. The obvious alternative interpretation is that the maximum is the result of a new injection of low energy SEPs, possibly from an event behind the east limb of the Sun (Ulysses was connected near the east limb at this time, as shown in Figure 1) and that the apparent velocity dispersion is a result of propagation effects.

[59] After day 331, aside from passage of a classic CIR with some low energy particle acceleration between days 333 and 336 (see Figure 3), the particle intensities decayed back to near-background levels by day 345.

4.4.2. Jovian Electrons Within the CME

[60] One remarkable feature during the passage of the CME, already noted in section 4.1 with reference to Figure 3 and now shown in more detail in Figure 11, is the abrupt intensity increase observed in the channels that normally respond primarily to 24–31 and 34–68 MeV protons at about 0600 UT on day 320. (In earlier figures, the 34–68 and 68–92 MeV proton channels, shown separately in Figure 11, have been presented as a combined 34–92 MeV channel. Angular sectoring is performed on the combined channel rather than the individual channels.) While these channels are normally dominated by protons, especially during SEP events, the logic that defines them permits electrons with energies of several MeV to contribute as well, as indicated in Figure 11. As confirmed by the absence of the signature in lower energy channels such as the 8–19 MeV proton channel from the LET telescope, which, by virtue of use of thinner detectors has greater immunity to electrons, and the good correlation with the HET 3–5 MeV electron channel (H7), which is designed to discriminate against protons [see *Simpson et al.*, 1992], this onset consists primarily of electrons. The electrons are almost certainly Jovian electrons. Close examination of the anisotropies from the combined channel in Figure 10e shows a brief period of anisotropic flow during the onset. These observations and observations of other anisotropic flows of Jovian electrons will be discussed in more detail in a subsequent paper (R. B. McKibben et al., manuscript in preparation, 2005).

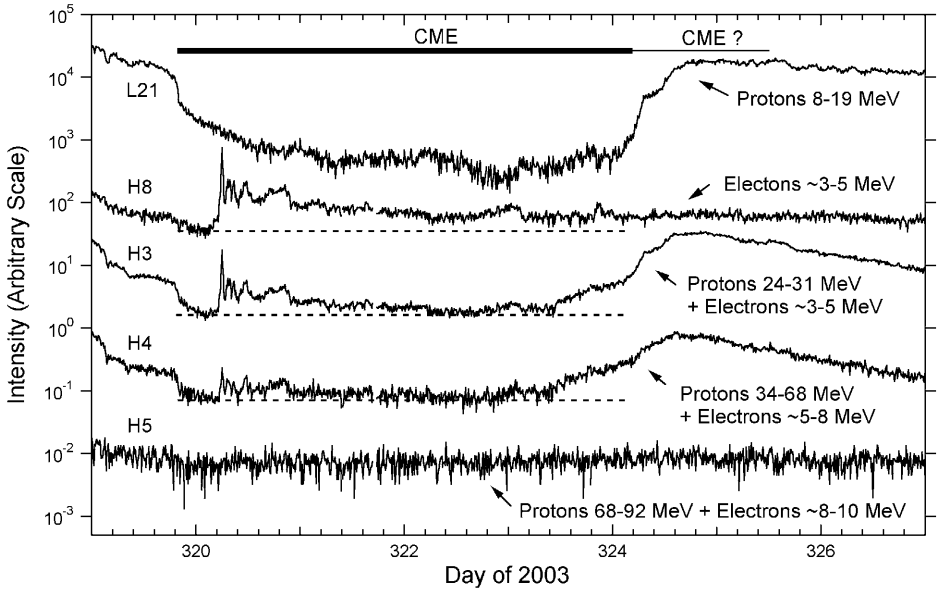

Figure 11. Blowup of the period affected by the large CME that passed Ulysses starting on day 319 to show the electron injection on day 320 and to highlight the relation of the CME boundaries to changes in the SEP intensity. Channels are identified both by the energy ranges of protons and electrons to which they respond, and by their channel name (L for LET, H for HET). Full logic requirements for the channels are given by *Simpson et al.* [1992].

[61] If the electrons are Jovian, the abrupt onset implies either a sudden release from Jupiter or sudden establishment of a good magnetic connection to Jupiter. At the time of the event, the spacecraft was 5.25 AU from the Sun at 5° heliographic latitude and 80.2° celestial longitude while, in the same coordinates, Jupiter was at 5.39 AU, −6.1° latitude and 79.7° longitude. Thus the spacecraft was within about 0.5° of longitude of Jupiter, 0.14 AU closer to the Sun, and about 11° separated in latitude. We suggest that it is possible that the electron onset corresponded to the impact of the CME on Jupiter's magnetosphere or to the entry of Jupiter into the magnetic structure of the CME. From the observation of bidirectional electron streaming throughout the CME, *de Koning et al.* [2005] conclude that closed magnetic field lines threaded the whole structure, which makes it likely that to be observed, the electrons must have been injected directly onto the field lines within the CME. At the time of onset, the measured solar wind speed was ∼940 km/s so that the radial separation of 0.14 AU between Ulysses and Jupiter would correspond to about 6.2 hours solar wind propagation time. Given the 11° separation in latitude, this is reasonably consistent with the observed delay of about 9.5 hours between Ulysses' entry into the CME and the sudden increase in Jovian electrons. Unfortunately, however, radio observations from the radio and plasma wave instrument on Ulysses showed no definitive signatures at the time of the onset (R.J. MacDowall, private communication, 2004). While this does not exclude a role for the CME interaction with Jupiter, it does not allow us to confirm the existence of a disturbance of Jupiter's magnetosphere associated with the onset.

[62] As shown by the dashed horizontal lines in Figure 11, set at the minimum intensity measured before the onset, the intensities remain slightly elevated for at least a day after the onset for ∼5–8 MeV electrons, and at least 2 days for ∼3–5 MeV electrons, suggesting, if the injection was impulsive rather than long-lasting, possible confinement and slow escape of the electrons from the CME.

5. Summary and Conclusions

[63] The comprehensive solar energetic particle measurements provided by the Ulysses COSPIN instruments during the October/November 2003 period from the heliographic equatorial zone near the orbit of Jupiter showed a very different picture of solar energetic particle propagation in the heliosphere than was shown during the near-solar-maximum period when Ulysses was at high latitudes. Instead of quick establishment of a uniform flux throughout the inner heliosphere, frequently referred to as the reservoir effect, observed near solar maximum [*McKibben et al.*, 2003], during the October/November 2003 period the particle populations were highly constrained and confined by the complex and evolving structure of the interplanetary medium. For both intensities and anisotropies, especially at energies below about 10 MeV, stream interfaces in CIRs appeared to serve as barriers, obstructing propagation of particles accelerated on one side from reaching the other. As a result, the time intensity profiles of the SEP fluxes were strongly affected by location of the spacecraft, and there was little commonality between the profiles observed at 1 AU and those observed at Ulysses. The reasons for this difference in behavior between the two periods is unclear, but may be related to solar cycle changes associated with the declining activity level and resultant simplification of the structure of the interplanetary medium. To the extent that similar multilocation observations are available from earlier cycles, a review of these observations would be

merited to see if similar differences have developed in previous cycles.

[64] In addition to the above, among interesting highlights of the events are the following:

[65] 1. During the onset of high-energy (>10 MeV) protons from the event on day 301, quasiperiodic fluctuations in the intensity and anisotropy of these protons appeared remarkably similar to the dropouts reported by *Mazur et al.* [2000] in observations of low-energy particles during impulsive events. These dropouts observed by Mazur et al. were interpreted as evidence for connection of flux tubes, adjacent at 1 AU, to significantly different locations on the Sun as a result of field line random walk. The present observations are on a greatly different scale, affecting particles at energies in excess of 92 MeV, and extending to 5.2 AU, where the length of the Parker spiral field was of the order of 13 AU at the time of observations.

[66] 2. There is evidence that solar energetic particles were effectively excluded from the interior of the extremely large CME that passed Ulysses between days 320 and 324, 2003. After passage of the CME, the intensities quickly returned to levels near those expected from continuing decay of the intensities observed prior to passage of the CME. It is, however unclear whether the particles observed after the CME represent a newly injected population, or whether a significant fraction of the particles are made up of the pre-existing population that became visible again once the spacecraft exited the zone of exclusion within the CME.

[67] 3. On day 319 there is evidence in both intensities and anisotropies for continuing acceleration of particles at 5.2 AU by the precursor shock of the large CME that began on day 320.

[68] 4. There is evidence of injection of electrons from Jupiter's magnetosphere, possibly triggered by impact of the CME, directly onto field lines inside the CME once the CME reached Jupiter. If this is correct, then the observations offer information about the shape of the CME on a scale of 11° of latitude. Since *de Koning et al.* [2005] conclude that the field had a closed flux rope structure. This raises interesting possibilities for studies of propagation within a CME.

[69] The October/November period provided an extraordinarily rich and complex series of events. Our effort in this paper has been primarily to give an overview of the observations that may be used as a basis for future study of these events. Already at this level, several interesting topics for further work are apparent. Of necessity, we have presented only a selection of the data channels available. We shall continue investigations ourselves, and stand ready to assist any and all who wish to delve more deeply into the available data sets from the COSPIN instruments.

[70] **Acknowledgments.** We gratefully acknowledge useful discussions with David Lario and with Robert MacDowall. Much of the COSPIN data shown in this paper is drawn from data sets prepared by COSPIN investigators and available on-line from the Ulysses Data System (UDS) at http://helio.estec.esa.nl/ulysses/. We particularly acknowledge the use of magnetic field and solar wind observations from the UDS. We are very grateful for the efforts of Cecil Tranquille in putting together, maintaining, and continually upgrading the UDS as a valuable resource not only for Ulysses investigators but for all of the heliospheric community. This work was supported in part by NASA/JPL contract 1247101.

[71] Arthur Richmond thanks Christina M. S. Cohen and David Lario for their assistance in evaluating this paper.

References

Crooker, N. U., et al. (1999), CIR morphology, turbulence, discontinuities, and energetic particles: Report of Working Group 2 of the ISSI Workshop on Corotating Interaction Regions, *Space Sci. Rev.*, *89*, 179–229.

de Koning, C. A., J. T. Steinberg, J. T. Gosling, D. B. Reisenfeld, R. M. Skoug, O. C. St. Cyr, M. L. Malayeri, A. Balogh, A. Rees, and D. J. McComas (2005), An unusually fast interplanetary coronal mass ejection observed by Ulysses at 5 AU on 15 November 2003, *J. Geophys. Res.*, *110*, A01102, doi:10.1029/2004JA010645.

Garcia-Munoz, M., G. M. Mason, and J. A. Simpson (1975), The isotopic composition of galactic cosmic-ray lithium, beryllium, and boron, *Astrophys. J. Lett.*, *201*, L145–148.

Lario, D., R. B. Decker, S. Livi, S. M. Krimigis, E. C. Roelof, C. T. Russell, and C. D. Fry (2005), Heliospheric energetic particle observations during the October–November 2003 events, *J. Geophys. Res.*, *110*, A09S11, doi:10.1029/2004JA010940.

Mazur, J. E., G. M. Mason, J. R. Dwyer, J. Giacalone, J. R. Jokipii, and E. C. Stone (2000), Interplanetary magnetic field line mixing deduced from impulsive solar flare particles, *Astrophys. J. Lett.*, *532*, L79–L82.

McKibben, R. B., et al. (2003), Ulysses COSPIN observations of cosmic rays and solar energetic particles from the south pole to the north pole of the Sun during solar maximum, *Ann. Geophys.*, *21*, 1217–1228.

Roelof, E. C., R. E. Gold, G. M. Simnett, S. J. Tappin, T. P. Armstrong, and L. J. Lanzerotti (1992), Low energy solar electrons and ions observed at Ulysses February–April, 1991: The inner heliosphere as particle reservoir, *Geophys. Res. Lett.*, *19*, 1243–1246.

Ruffolo, D., W. H. Matthaeus, and P. Chuychai (2003), Trapping of solar energetic particles by the small-scale topology of solar wind turbulence, *Astrophys. J. Lett.*, *597*, L169–L172.

Sanderson, T. R., G. Erdös, A. Balogh, R. J. Forsyth, R. G. Marsden, J. T. Gosling, J. L. Phillips, and C. Tranquille (2000), Effects of magnetic discontinuities on the propagation of energetic particles: Ulysses observations of the onset of the March 1991 solar particle event, *J. Geophys. Res.*, *104*, 18,275–18,283.

Sanderson, T. R., R. G. Marsden, C. Tranquille, S. Dalla, R. J. Forsyth, J. T. Gosling, and R. B. McKibben (2003), Propagation of energetic particles in the high-latitude high-speed solar wind, *Geophys. Res. Lett.*, *30*(19), 8036, doi:10.1029/2003GL017306.

Simpson, J. A., et al. (1992), The Ulysses cosmic ray and solar particle investigation, *Astron. Astrophys.*, *92*, 365–400.

Skoug, R. M., J. T. Gosling, J. T. Steinberg, D. J. McComas, C. W. Smith, N. F. Ness, Q. Hu, and L. F. Burlaga (2004), Extremely high speed solar wind: 29–30 October, 2003, *J. Geophys. Res.*, *109*, A09102, doi:10.1029/2004JA010494.

Stone, E. C., et al. (1998), The Solar Isotope Spectrometer for the Advanced Composition Explorer, *Space Sci. Rev.*, *86*, 357–408.

Tsurutani, B. T., et al. (2005), The October 28, 2003 extreme EUV solar flare and resultant extreme ionospheric effects: Comparison to other Halloween events and the Bastille Day event, *Geophys. Res. Lett.*, *32*, L03S09, doi:10.1029/2004GL021475.

Zimbardo, G., P. Pommois, and P. Veltri (2004), Magnetic flux tube evolution in solar wind anisotropic magnetic turbulence, *J. Geophys. Res.*, *109*, A02113, doi:10.1029/2003JA010162.

J. D. Anglin, Herzberg Institute of Astrophysics, National Research Council of Canada, 100 Sussex Drive, Ottawa, Ontario, Canada K1A 0R6. (dave.anglin@nrc.nrc-cnrc.gc.ca)

J. J. Connell, C. Lopate, and R. B. McKibben, Department of Physics and Space Science Center, University of New Hampshire, Morse Hall, 39 College Rd., Durham, NH 03824, USA. (connell@ulysses.sr.unh.edu; lopate@ulysses.sr.unh.edu; bruce.mckibben@unh.edu)

S. Dalla, Physics Department, UMIST, P.O. Box 88, Manchester M60 1QD, UK. (s.dalla@umist.ac.uk)

B. Heber, Physikalisches Institut, Universitaet Stuttgart, Pfaffenwaldring 57, D-70550 Stuttgart, Germany. (b.heber@physik.uni-stuttgart.de)

H. Kunow, Institut für Experimentelle und Angewandte Physik, Arbeitsgruppe für Extraterrestrische Physik, Christian Albrechts Universität, Leibnizstr. 1, D-24118 Kiel, Germany. (kunow@physik.uni-kiel.de)

R. G. Marsden and T. R. Sanderson, Research and Scientific Support Department, ESTEC, Postbus 299, 2200 AG, Noordwijk, Netherlands. (richard.marsden@esa.int; trevor.sanderson@esa.int)

M. Zhang, Department of Physics and Space Science, Florida Institute of Technology, 150 W. University Blvd., Melbourne, FL 32901-6975, USA. (mzhang@pss.fit.edu)